Research article JHEP|Reports

Heterogeneity in intrahepatic macrophage populations and druggable target expression in patients with steatotic liver disease-related fibrosis

Authors

Omar A. Saldarriaga, Timothy G. Wanninger, Esteban Arroyave, Joseph Gosnell, Santhoshi Krishnan, Morgan Oneka, Daniel Bao, Daniel E. Millian, Michael L. Kueht, Akshata Moghe, Jingjing Jiao, Jessica I. Sanchez, Heidi Spratt, Laura Beretta, Arvind Rao, Jared K. Burks, Heather L. Stevenson

Correspondence

hlsteven@utmb.edu (H.L. Stevenson).

Graphical abstract

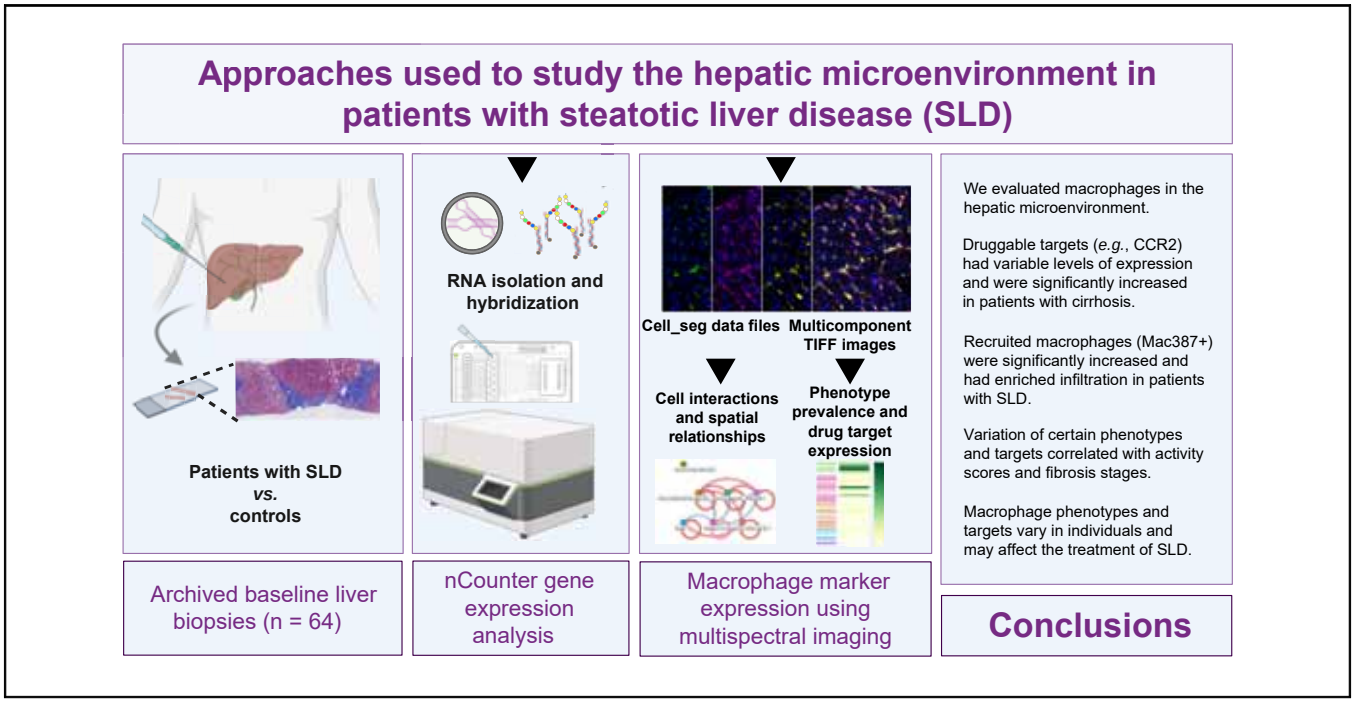

Highlights

- Molecular analysis and spectral imaging evaluated macrophages in patients with SLD.
- Druggable targets (*e.g.* CCR2) were significantly increased in patients with cirrhosis.
- Recruited macrophages (Mac387+) were increased and had enriched infiltration in SLD.
- Variation of certain phenotypes and targets correlated with activity scores and fibrosis stages.
- Macrophage phenotypes/targets vary in individuals and may affect the treatment of SLD.

Impact and implications

Appreciating individual differences within the hepatic microenvironment of patients with SLD may be paramount to developing effective treatments. These results may explain why such a small percentage of patients have responded to macrophage-targeting therapies and provide additional support for precision medicine-guided treatment of chronic liver diseases.

https://doi.org/10.1016/j.jhepr.2023.100958

Research article

JHEP|Reports

Heterogeneity in intrahepatic macrophage populations and druggable target expression in patients with steatotic liver disease-related fibrosis

Omar A. Saldarriaga,[1] Timothy G. Wanninger,[2] Esteban Arroyave,[1] Joseph Gosnell,[1] Santhoshi Krishnan,[3,4] Morgan Oneka,[3] Daniel Bao,[5] Daniel E. Millian,[1] Michael L. Kueht,[6] Akshata Moghe,[7] Jingjing Jiao,[8] Jessica I. Sanchez,[8] Heidi Spratt,[9] Laura Beretta,[8] Arvind Rao,[3,4,10,11,12] Jared K. Burks,[13] Heather L. Stevenson[1,*]

[1]Department of Pathology, University of Texas Medical Branch, Galveston, TX, USA; [2]Department of Microbiology and Immunology, University of Texas Medical Branch, Galveston, TX, USA; [3]Department of Computational Medicine and Bioinformatics, University of Michigan, Ann Arbor, MI, USA; [4]Department of Electrical and Computer Engineering, Rice University, Houston, TX, USA; [5]School of Medicine, University of Texas Medical Branch, Galveston, TX, USA; [6]Department of Surgery, University of Texas Medical Branch, Galveston, TX, USA; [7]Department of Internal Medicine, University of Texas Medical Branch, Galveston, TX, USA; [8]Department of Molecular and Cellular Oncology, University of Texas MD Anderson Cancer Center, Houston, TX, USA; [9]Department of Biostatistics and Data Science, University of Texas Medical Branch, Galveston, TX, USA; [10]Departmen of Radiation Oncology, University of Michigan, Ann Arbor, MI, USA; [11]Department of Biostatistics, University of Michigan, Ann Arbor, MI, USA; [12]Department of Biomedical Engineering, Rice University, Ann Arbor, MI, USA; [13]Department of Leukemia, University of Texas MD Anderson Cancer Center, Houston, TX, USA

JHEP Reports **2024.** https://doi.org/10.1016/j.jhepr.2023.100958

Background & Aims: Clinical trials for reducing fibrosis in steatotic liver disease (SLD) have targeted macrophages with variable results. We evaluated intrahepatic macrophages in patients with SLD to determine if activity scores or fibrosis stages influenced phenotypes and expression of druggable targets, such as CCR2 and galectin-3.

Methods: Liver biopsies from controls or patients with minimal or advanced fibrosis were subject to gene expression analysis using nCounter to determine differences in macrophage-related genes (n = 30). To investigate variability among individual patients, we compared additional biopsies by staining them with multiplex antibody panels (CD68/CD14/CD16/CD163/Mac387 or CD163/CCR2/galectin-3/Mac387) followed by spectral imaging and spatial analysis. Algorithms that utilize deep learning/artificial intelligence were applied to create cell cluster plots, phenotype profile maps, and to determine levels of protein expression (n = 34).

Results: Several genes known to be pro-fibrotic (*e.g.* CD206, TREM2, CD163, and ARG1) showed either no significant differences or significantly decreased with advanced fibrosis. Although marked variability in gene expression was observed in individual patients with cirrhosis, several druggable targets and their ligands (*e.g.* CCR2, CCR5, CCL2, CCL5, and LGALS3) were significantly increased when compared to patients with minimal fibrosis. Antibody panels identified populations that were significantly increased (*e.g.* Mac387+), decreased (*e.g.* CD14+), or enriched (*e.g.* interactions of Mac387) in patients that had progression of disease or advanced fibrosis. Despite heterogeneity in patients with SLD, several macrophage phenotypes and druggable targets showed a positive correlation with increasing NAFLD activity scores and fibrosis stages.

Conclusions: Patients with SLD have markedly varied macrophage- and druggable target-related gene and protein expression in their livers. Several patients had relatively high expression, while others were like controls. Overall, patients with more advanced disease had significantly higher expression of CCR2 and galectin-3 at both the gene and protein levels.

Impact and implications: Appreciating individual differences within the hepatic microenvironment of patients with SLD may be paramount to developing effective treatments. These results may explain why such a small percentage of patients have responded to macrophage-targeting therapies and provide additional support for precision medicine-guided treatment of chronic liver diseases.

Keywords: Cardiometabolic risk factors; Chemokines; Infiltrating monocytes; Inflammation; NanoString nCounter; Multispectral imaging; MASLD; Visiopharm.

Received 10 March 2023; received in revised form 18 August 2023; accepted 25 September 2023; available online 3 November 2023

* Corresponding author. Address: Department of Pathology, Director of Transplantation Pathology, The University of Texas Medical Branch, 712 Texas Ave., Clinical Services Wing - Room 5.506Q, Galveston, TX 77555-0416, USA. Tel.: +1-409-392-1568.

E-mail address: hlsteven@utmb.edu (H.L. Stevenson).

Introduction

Steatotic liver disease (SLD, previously non-alcoholic fatty liver disease [NAFLD])[1] is the leading cause of liver transplantation[2] and is the most common cause of chronic liver disease worldwide. It affects approximately 25–30% of the population, and is commonly associated with dyslipidaemia, obesity, metabolic disease, and type 2 diabetes.[3–5] SLD is the general term that includes all causes of hepatic steatosis, including metabolic

dysfunction, increased alcohol intake, drug-induced, and monogenic.[1] Metabolic dysfunction-associated SLD (now MASLD, previously NAFLD), includes patients that have hepatic steatosis and at least one of five cardiometabolic risk factors (*e.g.* BMI >25, type 2 diabetes mellitus, hypertension, or dyslipidaemia). Hepatic steatosis with evidence of associated hepatocellular injury, such as ballooning degeneration, is termed metabolic dysfunction-associated steatohepatitis (now MASH, previously non-alcoholic steatohepatitis [NASH]).[5] This newer multisociety consensus nomenclature also includes a category in addition to MASLD that allows the amount of alcohol use to be considered, termed MetALD.[1]

Under normal conditions, Kupffer cells maintain homeostasis and repair the liver after injury. However, in patients with steatohepatitis, Kupffer cell activation causes the recruitment of bone marrow-derived macrophages by the interaction of CCR2/CCL2 and CCR5/CCL5, promoting inflammation and the development of fibrosis.[6] Guillot *et al.*[7] recently reported that monocyte-derived macrophage accumulation is strongly associated with increased ductular reaction and was the most prominent immune-mediator of fibrosis progression, not only in patients with SLD, but also in those with primary sclerosing cholangitis and alcohol-related liver disease. Advanced fibrosis is the most critical histologic feature of SLD that independently predicts poor clinical outcomes and can lead to end-stage liver disease (ESLD) and hepatocellular carcinoma (HCC).[8,9] A recent analysis of normal liver using single-cell RNA sequencing revealed two CD68+ macrophage populations, one proinflammatory with increased Mac387 expression, and the other with immunoregulatory/tolerogenic functions and increased CD163 expression.[10] CD68 primarily identifies resident Kupffer cells, while Mac387 identifies recruited macrophages that infiltrate after injury in a CCL2-dependent manner.[11,12] CD163 has been reported as the prototypical 'M2' or pro-fibrotic macrophage marker that increases in number during hepatic fibrosis progression.[13] Activated hepatic stellate cells cause infiltration and differentiation of pro-fibrotic CD163+ macrophages via the CCL2/CCR2 pathway.[13] Circulating monocytes that enter the liver have also been characterised as inflammatory or anti-inflammatory based on the expression of CD14 or CD16, respectively.[14,15] However, less is known about these markers on human intrahepatic macrophages, although a CD14+CD16+ population has been shown to increase in the liver of mice with progression of fibrosis as a result of SLD.[16]

Therapies that target or inhibit pro-fibrotic macrophages have been used in clinical trials (*e.g.*, CENTAUR, AURORA, TANDEM, and GR-MD-02). Certain drugs, such as CCR2/CCR5 inhibitors (*e.g.* cenicriviroc) and galectin-3 (Gal3) antagonists (*e.g.* GR-MD-02), have shown promise in decreasing fibrosis in SLD.[6,17,18] For cenicriviroc, data from the CENTAUR study's year 1 analysis showed fibrosis improvement without impact on steatohepatitis in ∼20% of patients when compared with placebo. However, continued improvement in fibrosis was not observed at the end of year 2.[6,19,20] Previously, we showed that multispectral imaging can characterise numerous phenotypes of macrophages in patients with chronic liver diseases, including SLD.[21] For this study, we focused on fibrosis attributable to SLD and wanted to determine if certain patients had more numerous recruited macrophages in the liver and evaluated the expression of drug targets, such as CCR2 and galectin-3.

Materials and methods

Patients and liver biopsies

Studies were conducted on de-identified, archived liver biopsies from 2006 to 2022 and were approved by the University of Texas Medical Branch Institutional Review Board (IRB#13-0511 and 22-0223). Patients met the criteria to be included in the study if they had biopsy-proven SLD and a BMI of at least 25. For experiments where minimal and advanced fibrosis were compared, patients were matched by age, sex, and BMI. Minimal fibrosis included stages 1/4, and advanced fibrosis included stages 4/4. Inflammatory activity and fibrosis stages were determined by a board-certified pathologist using established criteria.[22] The number of patients included in each study are shown in Fig. 1 (Study Patient Sets 1–4). Demographics, clinical data, NAFLD activity scores (NAS), fibrosis stages, cardiometabolic criteria (CMC), and follow-up data (when available) are shown in the supplementary data file. Liver biopsies that showed minimal histopathologic findings and no steatosis that were collected from patients with normal liver enzymes at the time of the biopsy were used as controls.

RNA extraction and NanoString analysis

RNA was extracted from three unstained formalin-fixed, paraffin-embedded (FFPE) liver biopsy slides (cut at 3 μm) using the High Pure FFPET RNA Isolation kit (Roche, Mannheim, Germany). This kit is designed for isolating RNA from archived FFPE tissue blocks. RNA Concentrations were measured with a Qubit 2.0 fluorometer (Thermofisher, Waltham, MA, USA). To assess the quality of the extracted RNA, a bioanalyzer was used (RNA6000 pico-assay, Agilent, Santa Clara, CA, USA). Samples with a DV300 (a measure of RNA fragment size distribution) greater than 50% were selected for further analysis. This pre-analytic step ensured that the RNA was of sufficient quality for downstream processing. RNA samples (50 – 150 ng) were used for hybridization with expression profiling of ∼40 housekeeping genes and 730 immuno-oncology-related targets (PanCancer Immune Panel; NanoString Technologies, Seattle, WA, USA), including macrophage-related genes. The raw data (RCC files) were imported into nSolver software (NanoString Technologies), which performed comprehensive quality control checks on all the imported data generated throughout the protocol. The software assesses various aspects, including Imaging QC, Binding Density QC, and overall assay efficiency. As part of the nSolver analysis, positive controls were employed to evaluate assay performance. These controls serve as reference points for assessing the quality and reliability of the data obtained. Since the nCounter platform by NanoString is optimized for FFPE tissues, they have also conducted studies on different ages of specimens and found no differences, including whether fresh or FFPE tissues were used.[23] Data was then normalized and converted into $\log_2$-transformed data.

Multispectral analysis

Tissue blocks were stored at room temperature and sectioned immediately before multiplex staining, whenever possible. Slides that were unable to be stained within 1 week were stored at −80 °C in slide storage boxes with desiccant and wrapped with parafilm (to reduce moisture exposure). Multiplex panels (CD68/CD163/Mac387/CD14/CD16/DAPI); (CCR2/galectin-3/CD163/Mac387/DAPI) were optimised as previously described.[21] Staining was conducted manually or with the Ventana Discovery

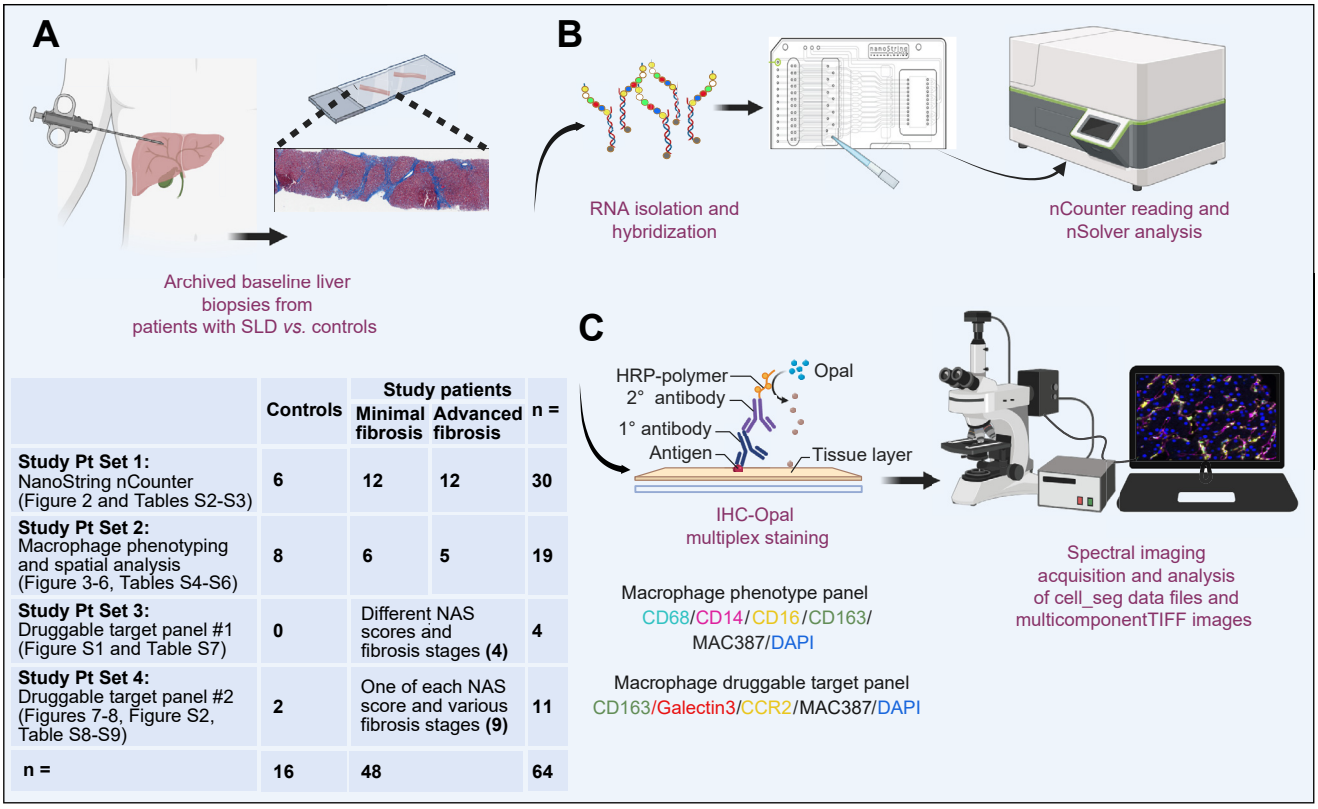

	Controls	Study patients: Minimal fibrosis	Study patients: Advanced fibrosis	n =
Study Pt Set 1: NanoString nCounter (Figure 2 and Tables S2-S3)	6	12	12	30
Study Pt Set 2: Macrophage phenotyping and spatial analysis (Figure 3-6, Tables S4-S6)	8	6	5	19
Study Pt Set 3: Druggable target panel #1 (Figure S1 and Table S7)	0	Different NAS scores and fibrosis stages **(4)**		4
Study Pt Set 4: Druggable target panel #2 (Figures 7-8, Figure S2, Table S8-S9)	2	One of each NAS score and various fibrosis stages **(9)**		11
n =	16	48		64

Fig. 1. Molecular and spectral imaging workflow. (A) Archived liver biopsy blocks from controls or patients with various stages of fibrosis attributable to SLD were selected. (B) Next, RNA was extracted from unstained slides for nCounter analysis. (C) For spectral imaging, slides were stained and scanned with the Vectra 3 Automated Quantitative Pathology Imaging system. Multicomponent TIFFs were analysed using Visiopharm to generate t-SNE plots and phenotype profile maps, and cell_seg files were used for UMAP, G-function, and Giotto analyses in collaboration with the University of Michigan. The table shows the number of patients included in each experiment. Created with BioRender.com. IHC, immunohistochemical; NAS, NAFLD activity scores; SLD, steatotic liver disease; t-SNE, t-distributed stochastic neighbour embedding; UMAP, uniform manifold approximation and projection.

Ultra (Roche Diagnostics, Indianapolis, IN, USA) as shown in Table S1. Images were acquired using the Vectra3 Quantitative Pathology Imaging system (Akoya Biosciences, Marlborough, MA, USA). Regions of interest (ROIs) were obtained from at least 50% of the surface area of each liver biopsy. Stamped areas for acquisition were 2 × 2 (1,338 μm × 1,000 μm) at a resolution of 0.5 μm (20×). Phenotypes were calculated as the percentage of the total cell population identified across all ROIs collected from each patient's liver biopsy (based on the nuclear stain DAPI) and included cells that were negative for all the markers.

Imaging and spatial analyses

For data analysis, first, multi-component TIFF images were exported from InForm (Akoya Biosciences) and analyzed with Visiopharm software (Visiopharm, Hoersholm, Denmark) using custom tissue detection, tissue segmentation, nuclear detection, and multiplex phenotyping applications and deep learning algorithms. Phenotype maps were used to determine location of phenotypes within the hepatic microenvironment and corresponding t-distributed stochastic neighbour embedding (t-SNE) plots were generated. Batch analysis was used to directly compare the minimal fibrosis group to the advanced fibrosis group, and then a separate algorithm was used to compare differences in the individual patients within each group.

Second, cell coordinates and intensity characteristics were extracted as cell_seg_data text files and provided to the imaging bioinformatics group at the University of Michigan. The heterogeneity and distribution of various cell phenotypes were determined using Uniform Manifold Approximation and Projection for Dimension Reduction (UMAP), a dimensional reduction technique similar to t-SNE for the visualization of high dimensional data.[24] Implementation and visualization of this workflow was done using MATLAB 2020a (MathWorks Inc., Natick, Massachusetts).[25] The spatial G-function is a nearest-neighbor-type cumulative distribution function used to quantify mixing and/or infiltration of a cell of interest around a reference cell.[26] Mathematically, it can be expressed as follows:

$$G_{(x,y)}(r) = 1 - e^{-\lambda_y \pi r^2}$$

Where the subscripts 'x' and 'y' indicate that the spatial distribution of cell type 'y' relative to cell type 'x' is being computed,' r' refers to the distance from the reference cell type, and λ_y is the overall density of cell type 'y' on the slide. Cell_seg files were also used for Giotto enrichment analysis. This was conducted first using cell locations to create a k-nearest neighbor graph, where k =4. In the neighbor graph, each node represents a cell, and edges between nodes indicate "interaction" between

the cells. Each cell is connected to its 3 nearest neighbors. Nodes are assigned to cell types based on the image data. To identify enriched or depleted interactions between cell type pairs, Giotto created a random permutation distribution by shuffling cell labels on the graph. It then calculated a *p* value for each cell-type pair by observing how often the simulated occurrence of edges between those cell types occurred in comparison to simulations. The G function and Giotto analysis were implemented using the spatstat and Giotto packages in R (R core team, 2021).[27]

Statistical analyses

Between-group analyses were performed using GraphPad Prism 9.5.0. Normal distribution of data was determined using D'Agostino-Pearson normality test. An unpaired t-test or Mann-Whitney test, as appropriate, with Holm-Sidak correction for multiple comparisons was used to compare the differences between two groups. A one-way ANOVA with Tukey's post-hoc test was used to compare the differences between three groups. A Pearson or Spearman test, as appropriate, was used for correlation assessments. The AUC of the computed G-function at selected 'r' values was computed to characterize infiltration. This workflow was implemented and visualised using R software.[28] Boxplot figures visualising the differences in significant groups were plotted in R using ggplot2.[29] p values <0.05 were considered statistically significant.

Results

The workflow is shown in Fig. 1. For the first set of analyses, we extracted RNA from whole liver tissue using unstained slides to determine differences in the expression of macrophage- and therapy-related genes relevant to the development of fibrosis and recent clinical trials.[6,11,13,18,30] Clinical data are shown in Table S2. Gene expression in matched patients with minimal and advanced fibrosis due to SLD are shown in the heatmap (Fig. 2A) and Table S3. Even though previous studies of other chronic liver diseases showed that CD68 significantly increased,[11] this study showed no significant difference in expression between controls or patients with minimal or advanced fibrosis due to SLD. Several genes that are known to be increased in hepatic fibrogenesis[13,31] showed no significant difference between the groups (*e.g.* CD206, TREM2) or significantly decreased with advancing fibrosis (*e.g.* CD163 and ARG1) (Fig. 2B). Targets of cenicriviroc (CCR2 and CCR5) and galactoarabino-24-rhannogalaturonan/GB1211 (galectin-3/LGALS3), as well as CCL2 and CCL5, were significantly increased in the patients with advanced fibrosis when compared to those with minimal fibrosis (Fig. 2B and Table S3). An important observation was the marked variability in the Log2 levels in the individual patients with SLD, especially in the groups with cirrhosis (Fig. 2B). These unexpected results prompted us to further evaluate macrophage phenotypes and expression of these targets *in situ* in the hepatic microenvironment with spectral imaging, an approach that preserves architecture and spatial context.

Archived blocks from patients with biopsy-proven SLD were again separated into minimal or advanced fibrosis groups and compared with controls. Clinical data at baseline biopsy are shown in Table S4. Representative multiplex images are shown in Fig. 3A–C. Visiopharm combines deep learning and artificial intelligence to provide accurate cell segmentation and multiplex phenotyping of tissue microenvironments. A phenotyping module analysed the cell population across all samples and fluorescent marker of interest to identify a unique cellular phenotype corresponding to a different colour for each cell (Fig. 3D–F). From these phenotypes, t-SNE plots (Fig. 3G–I) and phenotype profiles (Fig. 3J) were generated to compare different phenotypes in each group. The t-SNE plots showed unique phenotypic patterns in the different groups which were better identified and quantified in the corresponding phenotype profile map (Fig. 3J). We identified 25 different phenotypes with a prevalence greater than zero (cut-off: 0.1%) from the multiplex spectral images. Patients with advanced fibrosis due to SLD had significantly increased Mac387+ macrophages when compared with controls. However, no significant differences were observed between patients with minimal or advanced fibrosis. Several populations that included the presence of CD14 were significantly decreased in SLD. Again, no significant differences in these populations were observed in the patients with minimal or advanced fibrosis. Absolute numbers and details of the statistical comparisons are shown in Tables S5 and S6.

As no significant differences were observed in phenotypes between the groups of patients with minimal and advanced fibrosis attributable to SLD (Fig. 3), we hypothesised that heterogeneity may exist between individual patients. The prevalence of recruited monocyte-derived macrophages (Mac387+) was heterogeneous in both groups, with higher prevalence observed in a couple of patients within each group (Fig. 4). In the minimal fibrosis group, patients 27 and 29 had greater percentages of Mac387+ macrophages when compared with the other patients. Control 13 was the only patient that had a number above the cut-off we used in the generation of the Visiopharm heatmap. In the advanced fibrosis group, patient 32 had the highest percentage of CD14+ expression. Patient 34 had the greatest number of unique phenotypes, many of which were not present in the other patients in this group.

Next, instead of quantifying the different macrophage phenotypes in each of the patient groups, we evaluated their spatial relationships in the hepatic microenvironment. First, UMAPs, a dimension reduction tool, was used to visualise large, high-dimensional datasets and their local and global variations in cell biomarker expression (Fig. 5A–C). UMAP combines data from all images in each group while preserving the innate local and global relationships. Differential distribution of CD68+ and Mac387+ macrophages was observed with advanced fibrosis (Fig. 5D and E). Fig. 5F shows a representative G-function curve, where a steeper slope indicates more infiltration of the cell of interest near the reference phenotype at the given distance of observation. Fig. 5G compares the AUC of G-function curves for the Mac387+ *vs.* CD68+ phenotype pair. This was the only relationship for which a significant difference (p <0.01) was detected in the infiltration curves between the groups, with a bigger value indicative of increased infiltration of MAC387+ at smaller distances from CD68+. We also compared the interaction of phenotypes within the hepatic microenvironment using Giotto. Using X, Y coordinates of cell centroids and prior information about cell phenotypes, Giotto creates a nearest neighbour graph in the different groups using a custom-designed algorithm that allowed generation of a spatial analysis matrix plot (Fig. 5H). The y-axis shows each of the phenotype interactions detected and the x-axis (at the top) shows the different patient groups. Cell-pair enrichment interactions are shown in red, while cell-pair depletion interactions are shown in blue. Several enrichments were increased in patients with advanced fibrosis and these

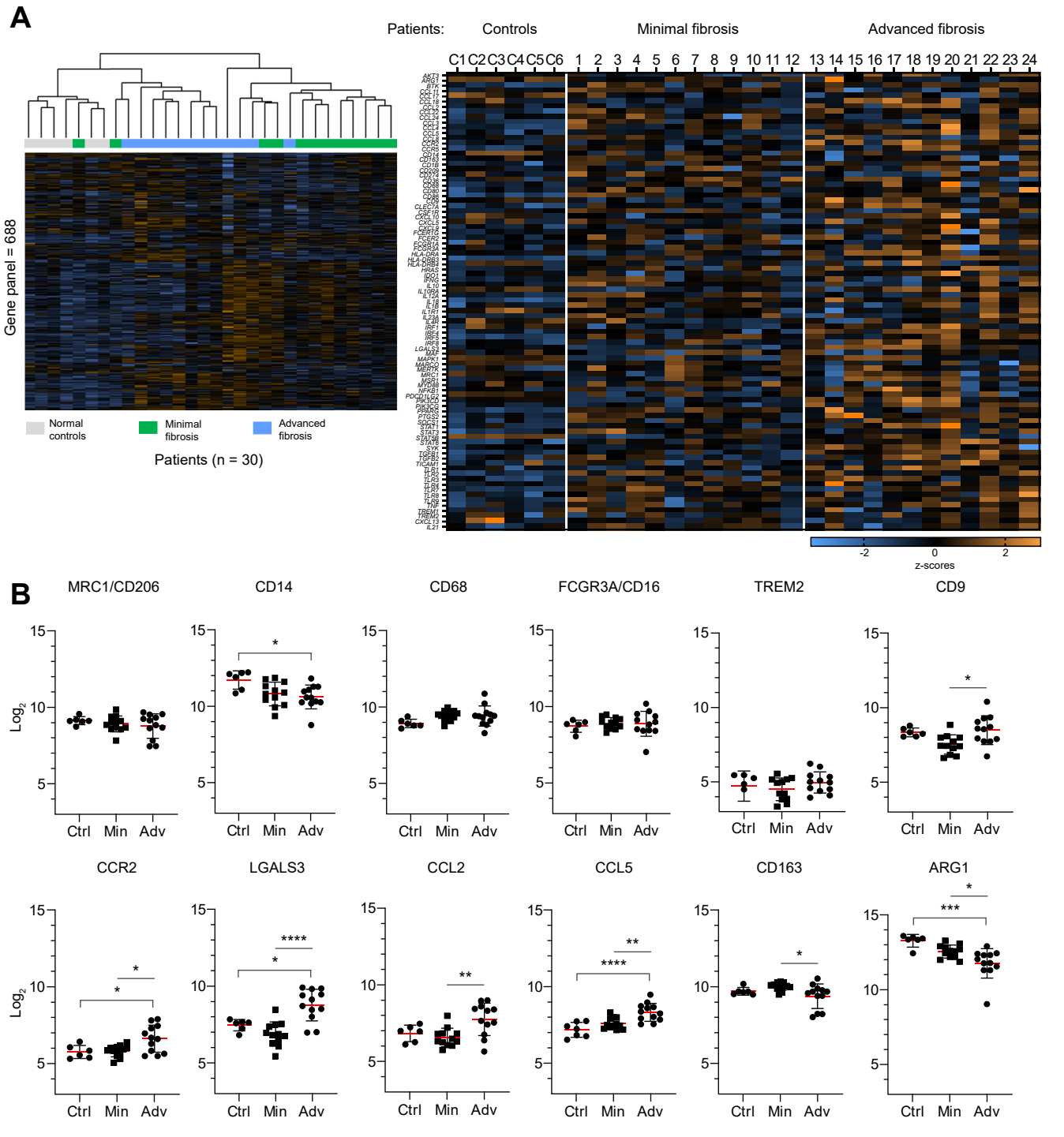

Fig. 2. nCounter analysis did not detect differences in several macrophage markers but showed significant differences in therapy-related markers. (A) Heatmaps with gene expression profiles from the different groups of liver biopsies showed independent clustering. Orange = high expression; blue = low expression. The panels to the right show macrophage-related gene expression. (B) Analyses between groups showed significant upregulation of CD9, CCR2, LGALS3, CCL2, and CCL5, and significant downregulation of CD14, CD163, and ARG1 with disease progression (see also Table S3). A one-way ANOVA with Tukey's correction was used to compare the groups; *p <0.05; **p <0.01; ***p <0.001; ****p <0.0001. A value of p <0.05 was considered significant. (See Tables S2 and S3 for additional details.) Adv, advanced fibrosis; Ctrl, controls; Min, minimal fibrosis.

included CD68+ and Mac387+ (Fig. 5H, red arrows). Three depletion interactions were identified in patients with advanced fibrosis when compared with those with minimal fibrosis (Fig. 5H, blue arrows). Next, we wanted to determine if certain patients had unique spatial interactions and evaluated each patient individually using Giotto. In Fig. 6A–D, each of the coloured dots represents a different macrophage phenotype and red or blue lines indicate cell-pair interactions. The phenotypes compared are shown in the color dots and the figure legend. Red lines indicate cell-pair interactions that were enriched, whereas

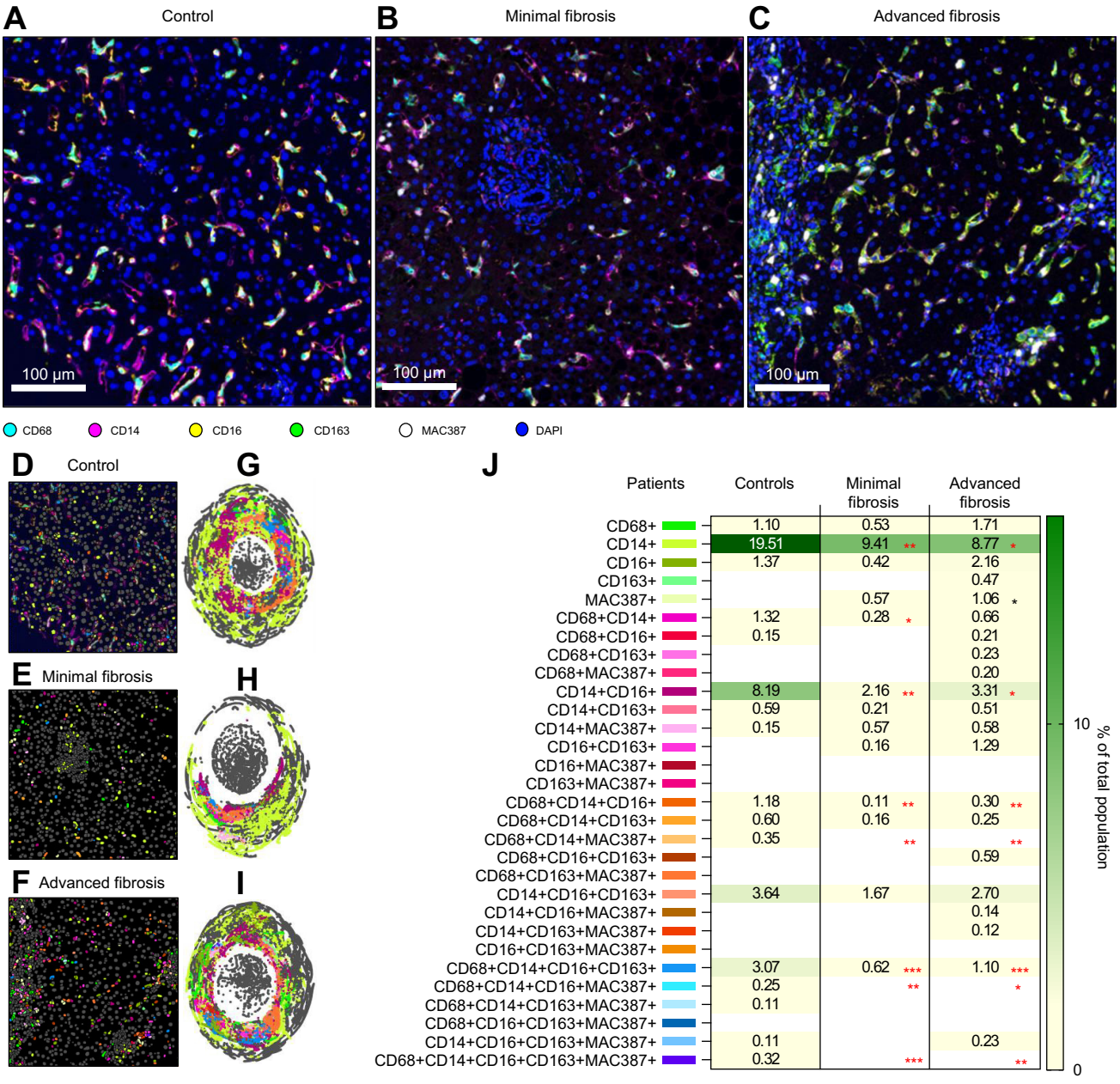

Fig. 3. Multispectral images, t-SNE plots, and phenotype profile maps comparing phenotypes of macrophages in SLD. (A–C) ROIs were collected from ~50% of each biopsy and representative images are shown. Visiopharm phenotype maps (D–F) with corresponding t-SNE plots (G–I) are shown. Each coloured dot designates a different phenotype that correlates with the colours in the phenotype profile map (J). Phenotypes were calculated as the percentage of the total cell population identified in all the ROIs collected from each patient's liver biopsy (using DAPI). A one-way ANOVA with Tukey's correction showed that patients with SLD had significantly different populations when compared with controls (*black = increased; red = decreased). Mac387+ macrophages were the only population that was significantly increased in patients with cirrhosis due to SLD. *p <0.05; **p <0.01; ***p <0.001. A value of p <0.05 was considered significant. Phenotype cut-off: 0.1%. (See Tables S4–S6 for additional details.) ROI, region of interest; SLD, steatotic liver disease; t-SNE, t-distributed stochastic neighbour embedding.

blue lines indicate cell-pair interactions that were depleted. Individual patients in both the minimal and advanced fibrosis groups had varied macrophage interactions. In the first comparisons (Fig. 6A and B), patients 27 and 29 were the only patients with minimal fibrosis that had enrichment of Mac387+ cells with Mac387+ cells (red arrows). In the advanced fibrosis group, patients 31 and 34 had more enrichment interactions than the group of patients with minimal fibrosis and the remaining patients in this group. Overall, patients with advanced fibrosis had more enrichment interactions, particularly patients 31, 32, and 34, who had several phenotypes enriched, more than other patients within this group, whereas patients 31, 33, and 34 had enrichment of Mac387+ (black arrows). In the second set of phenotype comparisons (Fig. 6C and D), patients 27 and 29 again showed enrichment of Mac387+ with Mac387+ macrophages. Follow-up data for these patients are shown in Table S4. Patients

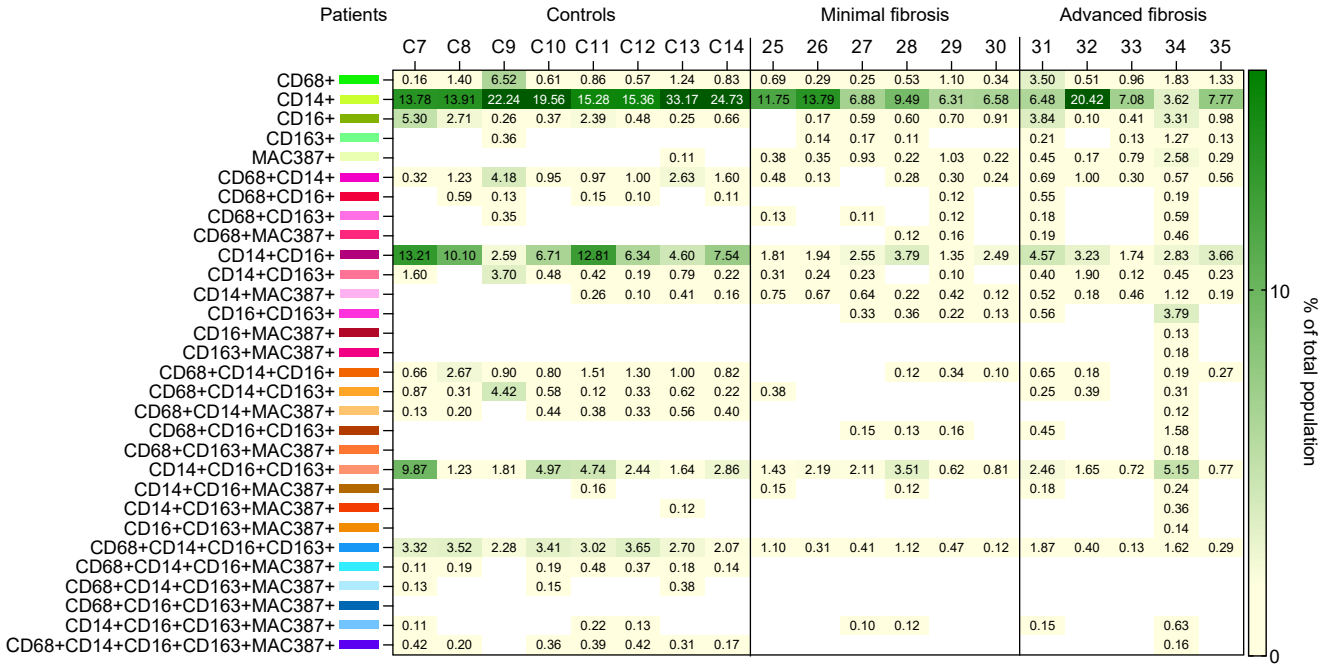

Fig. 4. Individual patients with SLD have variations in intrahepatic macrophage populations. Visiopharm algorithms were used to compare the prevalence of the phenotypes in the individual control and individual study patients with SLD from Fig. 3. Several identified phenotypes showed marked variability in the different groups. Patient 34 had numerous phenotypes, many of which were not identified in other patients. Phenotype cut-off: 0.1%. (See Tables S4–S6 for additional details.) SLD, steatotic liver disease.

27 and 29 later developed evidence of portal hypertension, including splenomegaly, thrombocytopaenia, and elevated partial thromboplastin time approximately 7.6 and 9.4 years later, respectively. Two of the patients with advanced fibrosis died approximately 3 and 4 years later, patient 32 from ESLD, and patient 34 from 'bowel rupture'. Patient 31 had compensated cirrhosis with features of portal hypertension.

As we observed variability in macrophage phenotypes that are known targets of emerging anti-fibrotic therapies in SLD (*e.g.* Mac387), we hypothesised that these patients may also have varied expression of therapeutic targets that could be detected. We randomly selected four liver biopsies (fibrosis stages 2–4/4) that were collected at our institution with confirmed SLD (one of these was from a patient that had both HCV and SLD), and used another multiplex panel containing CD163, galectin-3, CCR2, and Mac387 (Table S7 and Fig. S1). CCR2 and galectin-3 are two known druggable targets in clinical trials for the treatment of SLD-mediated fibrosis.[6,17,18] We separated all the images collected from each patient into portal tracts and lobules and phenotypes were calculated as the percentage of the total cell population in each patient's liver biopsy (based on nuclear staining with DAPI). Varied expression of CCR2 and galectin-3 was detected in patients with SLD. The patient that had the highest NAS (patient 37) had the highest expression of CD163 and galectin-3, while the patient with HCV in combination with SLD (patient 39) had the highest expression of CCR2 (Fig. S1). After this initial optimisation experiment, we ran this same panel on more patients, including two controls and nine different patients with varying NAS grades (Table S8 and Figs. 7 and 8). Even though we observed heterogeneity in individual patients, a positive correlation was detected between certain macrophage phenotypes and druggable targets with increased NAS (black asterisks) and fibrosis stages (red asterisks).

Discussion

SLD is increasing in prevalence and challenging to treat.[32,33] Several antifibrotic therapies in previous or ongoing clinical trials target intrahepatic macrophages (CENTAUR, AURORA, TANDEM, and GR-MD-02) without knowledge of the patient's underlying microenvironment. Initial trials for some of the most promising agents, such as cenicriviroc, terminated early because of lack of efficacy. Initial results of the CENTAUR trial showed that ~20% of patients had improvement of fibrosis (≥1 stage) without affecting steatosis or inflammatory activity associated with SLD at the end of year 1. At the end of year 2, no further improvement in fibrosis was observed.[6] Because cenicriviroc inhibits infiltration of pro-fibrotic macrophages into the liver via antagonism of CCR2/CCR5 and has been reported to decrease inflammation, steatosis, and fibrosis,[6,11,12,30,34,35] these results raised several questions. Why did patients with advanced fibrosis have a more pronounced response? Did all patients with biopsy-proven SLD have infiltrating macrophages in their livers? Why did such a small percentage of patients respond? Although serial liver biopsies were collected from patients at baseline, end of year 1, and end of year 2, these were only used to compare histologic changes (*i.e.* NAS and fibrosis stages).[6] We developed these studies to provide clues to these questions and to improve understanding of these complex cells within the human hepatic microenvironment.

First, we compared a group of matched patients with biopsy-confirmed SLD (Table S2) using NanoString nCounter (Fig. 2).

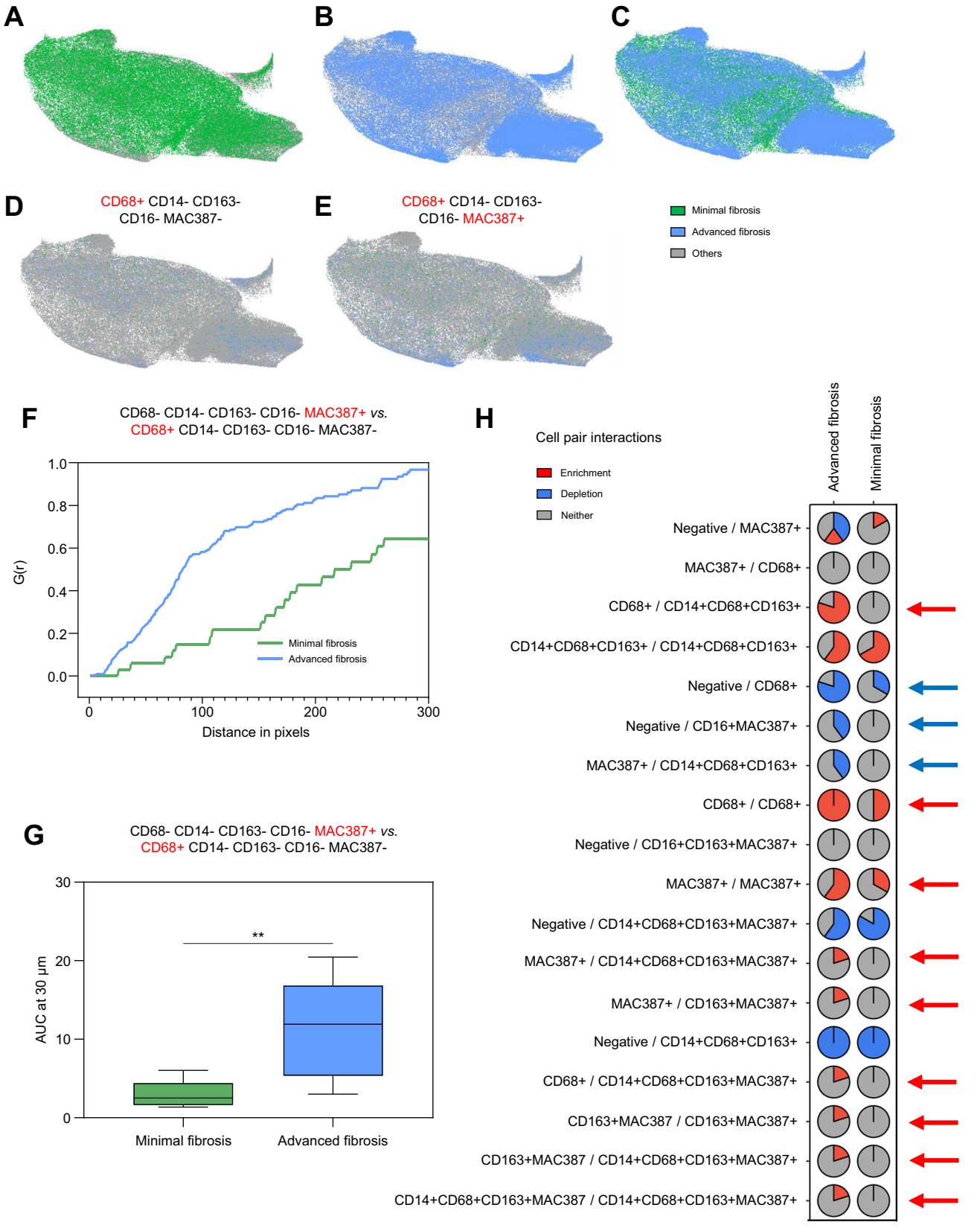

Fig. 5. Spatial analyses showed differences in infiltration between pairs of phenotypes. (A–E) UMAP compared variations in marker expression across datasets and visualised differences in CD68+ and CD68+/Mac387+ macrophages between the groups. (F–G) A representative AUC metric of the G-function that was used for estimating infiltration is shown. Infiltration between CD68+ and Mac387+ macrophages was significantly different between the two groups (p = 0.0012; Kruskal–Wallis). (H) Giotto compared the interactions of pairs of macrophage phenotypes and showed that several interactions involving CD68+ and Mac387+ were enriched in advanced fibrosis. Interaction type: red – enrichment; blue – depletion; grey – neither. (See Tables S4–S6 for additional details.) UMAP, uniform manifold approximation and projection.

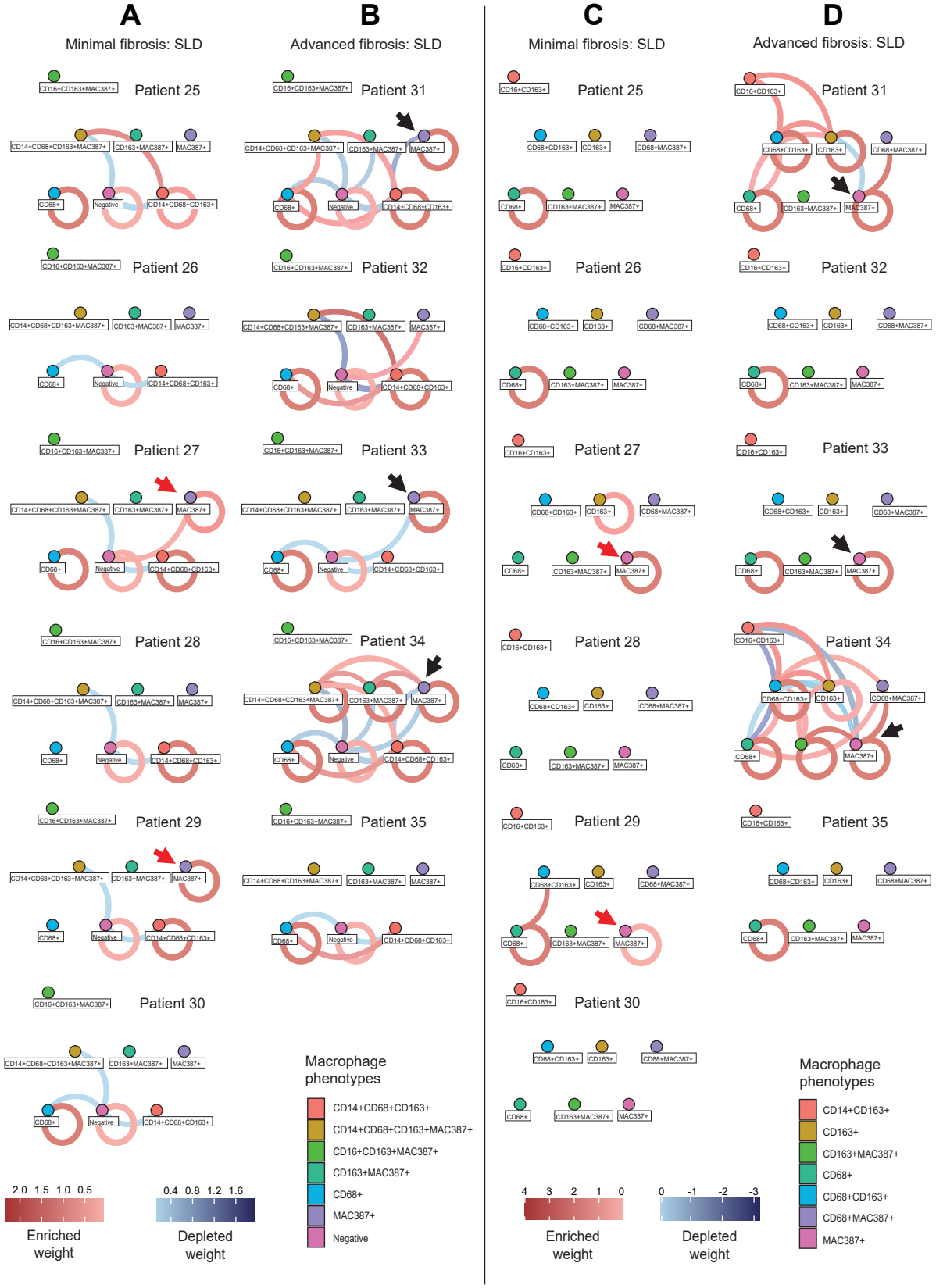

Fig. 6. Nearest-neighbour analysis showed variations among individual patients with SLD. Each network represents the cell-pair interactions from a single patient. Each coloured dot represents a different phenotype and red and blue lines represent enrichment and depletion, respectively (see legend). Patients 27 and 29 with minimal fibrosis, had enrichments of Mac387+ with Mac387+ macrophages (red arrows), an interaction that was common in advanced fibrosis (black arrows). Overall, within the advanced fibrosis group, patients 31, 32, and 34 had more enrichment interactions than the other patients, and patient 34 had the most. A–B and C–D show different cell-pair interactions as shown in the coloured legends. (See Tables S4–S6 for additional details.) SLD, steatotic liver disease.

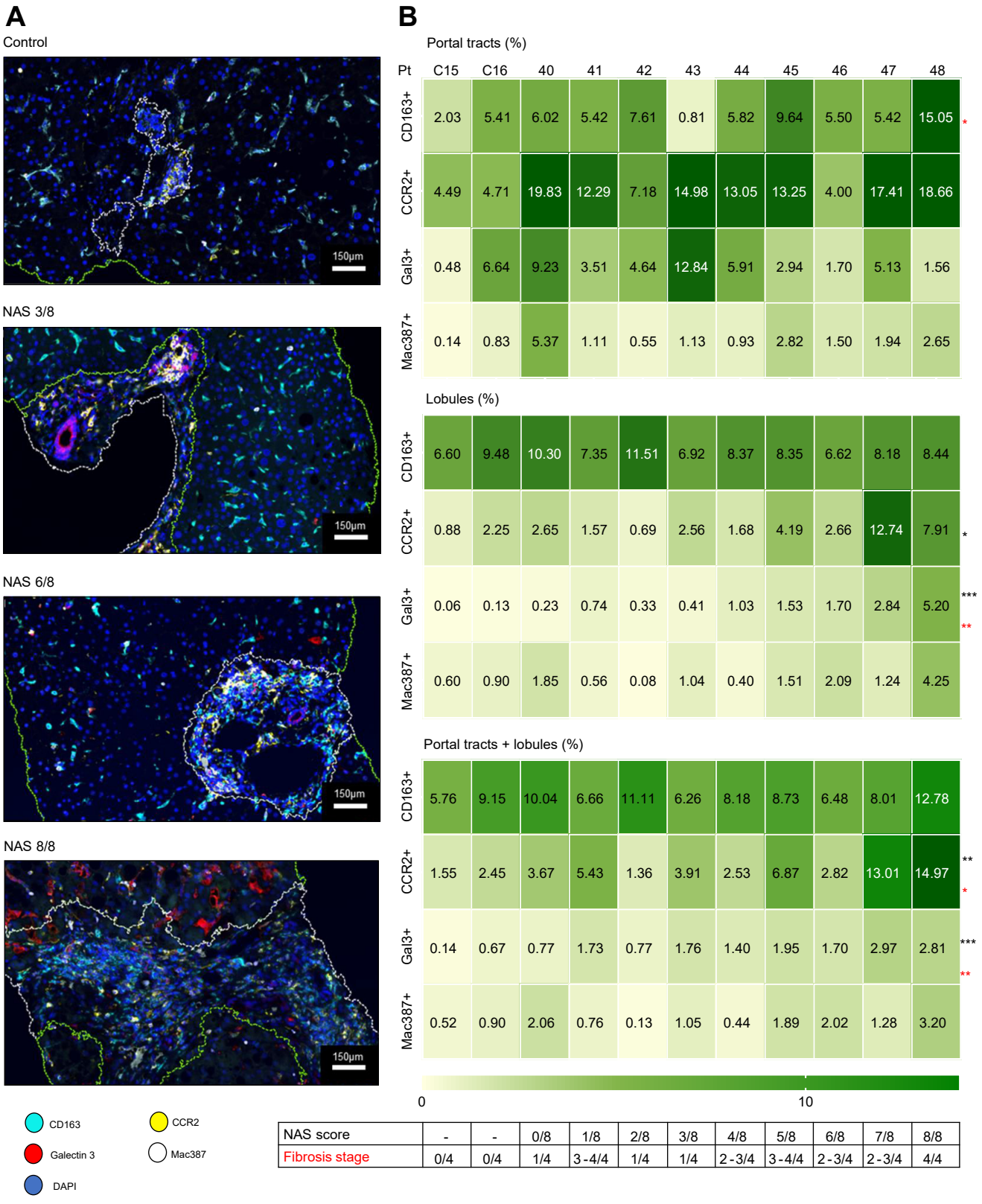

Fig. 7. Comparison of individual patients with SLD showed variation in macrophage phenotypes and druggable targets. (A) Liver biopsies from controls and patients with different NAFLD activity scores (NAS) were stained and multispectral images were segmented into regions using Visiopharm. Representative images are shown. (B) The percentage of marker-positive cells out of the total number of cells (DAPI+) in the segmented regions were calculated. Several patients had increased expression of CCR2 and galectin-3 when compared with other patients with higher NAS and fibrosis stages. Patient 40 had a previous biopsy 7 years earlier that showed a NAS of 4/8 and fibrosis stage of 2/4. Although individual variability was observed among patients, certain phenotypes and druggable targets

Gadd *et al.*[36] reported that CD68+ macrophages were increased in the portal tracts of patients with NAFLD and were one of the earliest changes detected and another study using digital spatial profiling revealed greater mRNA expression of CD68 in patients with advanced fibrosis caused by SLD.[37] However, we did not detect significant increases in several profibrotic macrophage-related genes (*e.g.* CD68, CD206, CD163, or ARG1). Several genes associated with macrophage-targeting therapies (*e.g.* CCL2, CCL5, CCR2, CCR5, and galectin-3/LGALS3) were significantly increased in patients with advanced fibrosis. Although results showed variability in both log2 levels (Fig. 2) and protein expression of several of these markers *in situ* in the hepatic microenvironment in patients with SLD (Figs. 7 and 8), molecular analysis still showed significantly higher expression in patients with advanced fibrosis (Fig. 2). However, homogenisation of liver tissue is unable to detect important differences in individual patients, phenotype percentages in the context of hepatic architecture, or significant spatial relationships. A recent study by Jiao *et al.*[38] showed that expression of pSTAT3 on segmented non-hepatocyte areas played a key role in fibrogenesis and results were dependent on spatial context. Guillot *et al.*[7] also recently spatially resolved the hepatic microenvironment and determined that loss of hepatocytes and ductular reaction were associated with monocyte-derived macrophage infiltration and fibrosis progression in several chronic liver diseases, including NAFLD/SLD. Because of these results, additional experiments were conducted using spectral imaging; an approach that can analyse macrophage populations *in situ* with preservation of hepatic architecture.

As cenicriviroc resulted in a more pronounced response in patients with advanced fibrosis,[6] we hypothesised that patients with bridging fibrosis/cirrhosis would have increased prevalence of infiltrating macrophages, enhanced spatial relationships, enrichment of macrophage phenotypes, and higher expression of treatment targets, such as CCR2. As a small percentage of patients with SLD showed improvement after cenicriviroc treatment, we also predicted that there would be variability in prevalence of certain phenotypes and marker expression between individual patients. Interestingly, both groups of patients with SLD showed significantly increased percentages of recruited macrophages, but significant upregulation (*i.e.* the Mac387+ phenotype) was only seen in patients with advanced fibrosis compared to controls. Moreover, no significant difference was observed between the two groups of patients with SLD because of the presence of substantial heterogeneity in individual patients (Figs. 3 and 4). CD68+ and Mac387+ phenotypes have also been shown to be increased in patients with chronic liver disease when compared with controls.[11] Although we expected to see some variability in the prevalence of Mac387 expression in the individual patients, we did not expect two patients with minimal fibrosis (patients 27 and 29) to have a higher prevalence of infiltrating macrophages than most patients with advanced fibrosis (see Fig. 4).

As spatial analysis of the tumour microenvironment has predicted drug efficacy and clinical outcome in patients with HCC and cholangiocarcinoma, respectively,[39,40] we applied similar approaches to patients with SLD. We used UMAP, G-function, and Giotto to quantify mixing and/or infiltration of macrophage phenotypes. The interaction of Mac387+ and CD68+ cells, either with each other or with other markers, was significantly increased in the patients with advanced fibrosis (see Fig. 5). Huang *et al.*[11] showed that these two phenotypes increase in patients with chronic liver disease. It seems obvious that cells that are increased in number in a tissue site will have more opportunities to be near one another. However, we evaluated spatial relationships of all 25 phenotypes identified in this study, and only the interaction between Mac387+ and CD68+ macrophages reached statistical significance (see Fig. 5).

Analysis of individual patients with minimal fibrosis showed that only two patients had increased enrichment of Mac387+ macrophages (Fig. 6A and C, patients 27 and 29), and these patients later developed portal hypertension (see Fig. 6 and Table S4). Patients 33 and 34 with advanced fibrosis also had a higher prevalence of Mac387+ cells when compared with other patients (Fig. 4). Patient 32 was deceased because of ESLD and baseline biopsy did not show increased prevalence of the macrophage phenotypes evaluated. Patient 34 had a high prevalence of numerous phenotypes within the liver and was reported deceased from a bowel rupture attributable to underlying ischaemic colitis, 4.9 years after baseline biopsy (see Fig. 4 and Table S4). These interactions deserve further investigation since Mac387+ cells are known to mediate hepatic fibrosis and are one of the main targets of drugs such as cenicriviroc.

The amount of heterogeneity among individual patients with SLD, particularly with phenotypes known to be profibrotic (*e.g.* Mac387+ and CD163+), prompted us to evaluate the next four patients diagnosed with SLD by liver biopsy. We conducted spectral imaging analysis in addition to routine NAS grading and fibrosis staging (Table S7 and Fig. S1). Analysis of a larger group of patients showed similar results with increased expression correlating with increased NAS and fibrosis stages (Figs. 7 and 8, Table S8, Fig. S2, and Table S9). However, PD-L1+ host cells within the hepatic microenvironment are more likely to respond to immunotherapy against this target, and a recent study by Lu *et al.*[41] in *Gut* reported that selective modulation of macrophages restores antitumoral properties in patients with HCC. If macrophages can be 'selectively modified' in the livers of patients that already have cancer, they most certainly can be modified earlier in the course of the disease where poor outcomes such as cirrhosis and HCC have a chance of being prevented.

A major strength of this study is that we analysed the human liver microenvironment *in situ* in biopsies from real patients with SLD. Many studies of the hepatic microenvironment and immune response have been conducted *in vitro* and in mouse models, including several that led to cenicriviroc therapy for SLD.[42] It is well known that mice differ from humans.[43,44] An elegant comparative study by Jiang *et al.*[44] compared mouse, human, and humanised mouse livers in fatty liver disease, and showed that gene expression in mice and humans is quite different, with only

showed a positive correlation with NAS scores and fibrosis stages. Pearson or Spearman tests were used, accordingly, to correlate phenotypic markers with NAS and fibrosis stages in the different regions. Red asterisks = correlation with fibrosis; black asterisks = correlation with NAS. *p <0.05; **p <0.01; ***p <0.001. A value of p <0.05 was considered significant. Created with GraphPad Prism (See Table S9 and Fig. S2 for additional details.) SLD, steatotic liver disease.

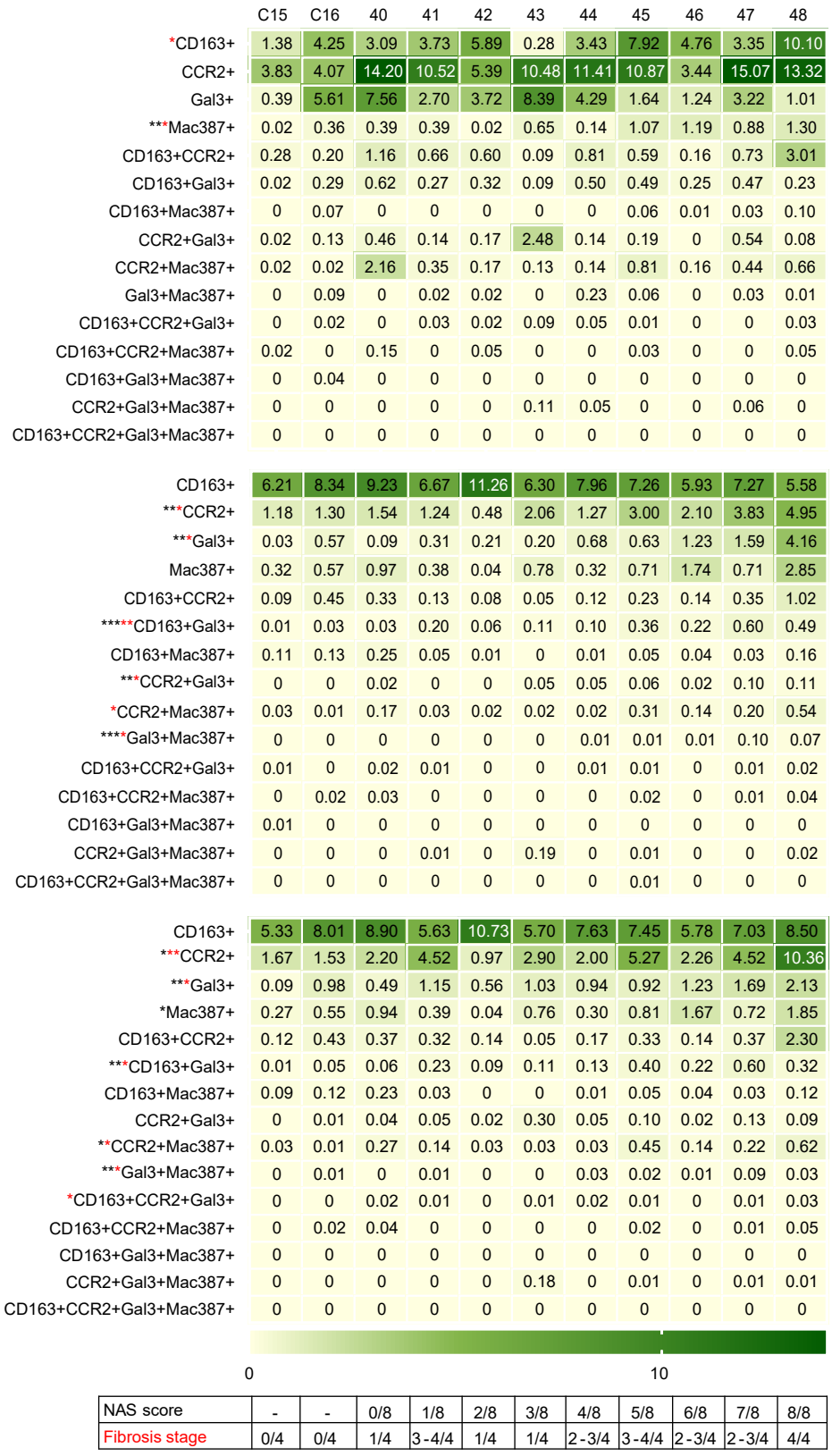

Fig. 8. Individual patients with SLD have unique phenotypes that express CCR2 and galectin-3 (Gal3). A custom Visiopharm algorithm compared the prevalence of phenotypes in the patients from Fig. 7. Although individual variability was observed among patients, certain phenotypes and druggable targets showed a correlation with NAS scores and fibrosis stages. Pearson or Spearman tests were used, accordingly, to correlate phenotypic markers with NAS and fibrosis stages in the different regions. Red asterisks = correlation with fibrosis; black asterisks = correlation with NAS. *p <0.05; **p <0.01; ***p <0.001. A value of p <0.05 was considered significant. Created with GraphPad Prism (See Table S9 and Fig. S2 for additional details.) NAS, NAFLD activity scores; SLD, steatotic liver disease.

1,524 genes commonly regulated. In addition, it takes years to develop cirrhosis and HCC when you have chronic liver disease, so replicating the duration of the disease is not feasible when using animal models. Studies in humans, although more translational and often more clinically relevant, also pose challenges. First, mechanistic studies are nearly impossible, whereas they are common in mouse models. Second, as we observed in these patients, macrophages within the hepatic microenvironment vary substantially and each patient has their own unique populations.

In summary, if we can learn how to modulate the hepatic microenvironment earlier during disease before cirrhosis or HCC develop, we may be able to prevent poor outcomes before it is too late to intervene. We hope the results of this study will inspire development of more targeted, translational approaches for the treatment of SLD and other chronic medical liver diseases.

Abbreviations

ADV, advanced fibrosis; ALP, alkaline phosphatase; ALT, alanine transaminase; AST, aspartate aminotransferase; ESLD, end-stage liver disease; FFPE, formalin-fixed, paraffin-embedded; Gal3, galectin-3; HCC, hepatocellular carcinoma; MASH, metabolic dysfunction-associated steatohepatitis; MASLD, metabolic dysfunction-associated steatotic liver disease; MetALD, MASLD with alcohol intake; MIN, minimal fibrosis; NAFLD, non-alcoholic fatty liver disease (now MASLD); NAS, NAFLD activity scores; NASH, non-alcoholic steatohepatitis; SLD, steatotic liver disease; ROI, region of interest; t-SNE, t-distributed stochastic neighbour embedding; UMAP, uniform manifold approximation and projection; BMI, body mass index; CMC, cardiometabolic criteria; HCV, hepatitis C virus.

Financial support

The authors acknowledge and thank their grant funding sources. OAS, EA, SK, MO, HS, LB, AR, and HLS, were partially supported by a R01 from the National Institute of Diabetes and Digestive and Kidney Diseases (NIDDK) (1R01DK125730-01A1-3). OAS and HSL were also supported by a Moody Endowment Grant (2014-07; LIME 19016). Initial optimisation studies were supported in part by the National Center for Advancing Translational Sciences (NCATS) and the Clinical and Translational Science Award (CTSA) Grant KL2 Scholars Program (KL2TR001441). The Vectra 3 microscope was purchased with funds from the University of Texas Science and Technology Acquisition and Retention (STARs) Program. AR and SK were supported by the Cancer Center Support Grant (CCSG) Bioinformatics Shared Resource (5 P30 CA046592), a gift from Agilent Technologies, and a Precision Health Investigator award from the University of Michigan. SK and AR were partially supported by the NCI Grant R37-CA214955. SK and AR were also partially supported by The University of Michigan startup institutional research funds. SK and AR were also supported by a Research Scholar Grant from the American Cancer Society (RSG-16-005-01). MO was supported by the Advanced Proteome Informatics of Cancer Training Grant (T32 CA140044).

Conflicts of interest

HSL and OAS have a filed patent titled “Systems and methods for spectral imaging characterization of macrophages for use in personalization of targeted therapies to prevent fibrosis development in patients with chronic liver disease." (Board or Regents, The University of Texas System, United States, Galveston, Texas; Pub. No: US 20210293814.) AR serves as a member of Voxel Analytics LLC and consults for Tempus Labs Inc, and Tata Consultancy Services Ltd. The remaining authors who have taken part in this study declared that they do not have anything to disclose regarding funding or conflict of interest with respect to this manuscript.

Please refer to the accompanying ICMJE disclosure forms for further details.

Authors’ contributions

Data curation: OAS, JG. Formal analysis: OAS, TGW, DEM, DB, EA, SK, MO, AR, HS. Methodology: OAS, EA, JJ, JIS, LB, EA. Software: TGW, DEM, DB, SK, MO, AR. Validation: EA. Resources: JKB. Project administration, Conceptualisation, Supervision: HLS. Writing – original draft: OAS. Writing – review & editing: OAS, MK, AM, HLS. Reviewed the manuscript: all authors.

Data availability statement

All data relevant to the study are included in the article or were uploaded in the supplementary materials.

Acknowledgements

Dr Brit Boehmer and Justin Major from Visiopharm assisted with training and data analysis. Sam Diaz de Leon and Blanca Hernandez provided secretarial support and assistance with obtaining the archived liver biopsy tissue blocks. Liliana Cadavid assisted with graphic ilustration. We thank Drs John Vierling and Frank Tacke for their expert feedback regarding the figures in this paper. Shana White, the clinical study coordinator, assisted with chart review, IRB approval, and demographic information.

Supplementary data

Supplementary data to this article can be found online at https://doi.org/10.1016/j.jhepr.2023.100958.

References

Author names in bold designate shared co-first authorship

[1] Rinella ME, Lazarus JV, Ratziu V, Francque SM, Sanyal AJ, Kanwal F, et al. A multi-society Delphi consensus statement on new fatty liver disease nomenclature. Hepatology 2023. Published online ahead of print 24 Jun.

[2] **Noureddin M**, **Vipani A**, Bresee C, Todo T, Kim IK, Alkhouri N, et al. NASH leading cause of liver transplant in women: updated analysis of indications for liver transplant and ethnic and gender variances. Am J Gastroenterol 2018;113:1649–1659.

[3] Laursen TL, Mellemkjær A, Møller HJ, Grønbæk H, Kazankov K. Spotlight on liver macrophages for halting injury and progression in nonalcoholic fatty liver disease. Expert Opin Ther Targets 2022;26:697–705.

[4] Sheka AC, Adeyi O, Thompson J, Hameed B, Crawford PA, Ikramuddin S. Nonalcoholic steatohepatitis: a review. JAMA 2020;323:1175–1183.

[5] Chalasani N, Younossi Z, Lavine JE, Charlton M, Cusi K, Rinella M, et al. The diagnosis and management of nonalcoholic fatty liver disease: practice guidance from the American Association for the Study of Liver Diseases. Hepatology 2018;67:328–357.

[6] Ratziu V, Sanyal A, Harrison SA, Wong VWS, Francque S, Goodman Z, et al. Cenicriviroc treatment for adults with nonalcoholic steatohepatitis and fibrosis: final analysis of the phase 2b CENTAUR study. Hepatology 2020;72:892–905.

[7] Guillot A, Winkler M, Silva Afonso M, Aggarwal A, Lopez D, Berger H, et al. Mapping the hepatic immune landscape identifies monocytic macrophages as key drivers of steatohepatitis and cholangiopathy progression. Hepatology 2023;78:150–166.

[8] Dulai PS, Singh S, Patel J, Soni M, Prokop LJ, Younossi Z, et al. Increased risk of mortality by fibrosis stage in nonalcoholic fatty liver disease: systematic review and meta-analysis. Hepatology 2017;65:1557–1565.

[9] Vilar-Gomez E, Calzadilla-Bertot L, Wong VWS, Castellanos M, Aller-de la Fuente R, Metwally M, et al. Fibrosis severity as a determinant of cause-specific mortality in patients with advanced nonalcoholic fatty liver disease: a multi-national cohort study. Gastroenterology 2018;155:443–457.e17.

[10] **MacParland SA**, **Liu JC**, **Ma XZ**, Innes BT, Bartczak AM, Gage BK, et al. Single cell RNA sequencing of human liver reveals distinct intrahepatic macrophage populations. Nat Commun 2018;9:4383.

[11] Huang R, Wu H, Liu Y, Yang C, Pan Z, Xia J, et al. Increase of infiltrating monocytes in the livers of patients with chronic liver diseases. Discov Med 2016;21:25–33.

[12] Antoniades CG, Quaglia A, Taams LS, Mitry RR, Hussain M, Abeles R, et al. Source and characterization of hepatic macrophages in acetaminophen-induced acute liver failure in humans. Hepatology 2012;56:735–746.

[13] **Xi S**, **Zheng X**, Li X, Jiang Y, Wu Y, Gong J, et al. Activated hepatic stellate cells induce infiltration and formation of CD163(+) macrophages via CCL2/CCR2 pathway. Front Med (Lausanne) 2021;8:627927.

[14] Wermuth PJ, Jimenez SA. The significance of macrophage polarization subtypes for animal models of tissue fibrosis and human fibrotic diseases. Clin Transl Med 2015;4:2.

[15] Liaskou E, Zimmermann HW, Li KK, Oo YH, Suresh S, Stamataki Z, et al. Monocyte subsets in human liver disease show distinct phenotypic and functional characteristics. Hepatology 2013;57:385–398.

[16] Fukushima H, Kono H, Hirayama K, Akazawa Y, Nakata Y, Wakana H, et al. Changes in function and dynamics in hepatic and splenic macrophages in non-alcoholic fatty liver disease. Clin Exp Gastroenterol 2020;13:305–314.

[17] Patikorn C, Veettil SK, Phisalprapa P, Pham T, Kowdley KV, Chaiyakunapruk N. Horizon scanning of therapeutic modalities for nonalcoholic steatohepatitis. Ann Hepatol 2021;24:100315.

[18] Harrison SA, Marri SR, Chalasani N, Kohli R, Aronstein W, Thompson GA, et al. GR-MD-02, a galectin-3 inhibitor, vs. placebo in patients having non-alcoholic steatohepatitis with advanced fibrosis. Aliment Pharmacol Ther 2016;44:1183–1198.

[19] **Friedman SL**, **Ratziu V**, Harrison SA, Abdelmalek MF, Aithal GP, Caballeria J, et al. A randomized, placebo-controlled trial of cenicriviroc for treatment of nonalcoholic steatohepatitis with fibrosis. Hepatology 2018;67:1754–1767.

[20] Friedman S, Sanyal A, Goodman Z, Lefebvre E, Gottwald M, Fischer L, et al. Efficacy and safety study of cenicriviroc for the treatment of non-alcoholic steatohepatitis in adult subjects with liver fibrosis: CENTAUR Phase 2b study design. Contemp Clin Trials 2016;47:356–365.

[21] Saldarriaga OA, Freiberg B, Krishnan S, Rao A, Burks J, Booth AL, et al. Multispectral imaging enables characterization of intrahepatic macrophages in patients with chronic liver disease. Hepatol Commun 2020;4:708–723.

[22] Kleiner DE, Brunt EM, Van Natta M, Behling C, Contos MJ, Cummings OW, et al. Design and validation of a histological scoring system for nonalcoholic fatty liver disease. Hepatology 2005;41:1313–1321.

[23] Zheng CM, Piao XM, Byun YJ, et al. Study on the use of Nanostring nCounter to analyze RNA extracted from formalin-fixed-paraffin-embedded and fresh frozen bladder cancer tissues [Cancer Genetics 268-269 (2022) 137-143]. Cancer Genet Jan 2023;31:270–271.

[24] McInnes L, Healy J. Uniform manifold approximation and projection for dimension reduction. 2018; http://arxiv.org/abs/1802.03426.

[25] Meehan Connor, Jonathan Ebrahimian WM, Meehan Stephen. Uniform manifold approximation and projection (UMAP). MATLAB Central File Exchange; 2021.

[26] **Carstens JL**, **Correa de Sampaio P**, Yang D, et al. Spatial computation of intratumoral T cells correlates with survival of patients with pancreatic cancer. Nat Commun Apr 27 2017;8:15095.

[27] Baddeley A, Rubak E, Turner R. Spatial point patterns: methodology and applications with R. First Edition ed. Chapman & Hall/CRC Interdisciplinary Statistics; 2015.

[28] Team RCR. A language and environment for statistical computing. Vienna, Austria: R Foundation for Statistical Computing; 2014; http://www.R-project.org/.

[29] Wickham H. ggplot2: elegant graphics for data analysis. New York: Springer; 2009.

[30] Anstee QM, Neuschwander-Tetri BA, Wong VW, Abdelmalek MF, Younossi ZM, Yuan J, et al. Cenicriviroc for the treatment of liver fibrosis in adults with nonalcoholic steatohepatitis: AURORA Phase 3 study design. Contemp Clin Trials 2020;89:105922.

[31] Pastore M, Caligiuri A, Raggi C, Navari N, Piombanti B, Di Maira G, et al. Macrophage MerTK promotes profibrogenic cross-talk with hepatic stellate cells via soluble mediators. JHEP Rep 2022;4:100444.

[32] Hernandez Roman J, Patel S. Why do lifestyle recommendations fail in most patients with nonalcoholic fatty liver disease? Gastroenterol Clin North Am 2020;49:95–104.

[33] Zelber-Sagi S. Dietary treatment for NAFLD: new clinical and epidemiological evidence and updated recommendations. Semin Liver Dis 2021;41:248–262.

[34] Seki E, de Minicis S, Inokuchi S, Taura K, Miyai K, VanRooijen N, et al. CCR2 promotes hepatic fibrosis in mice. Hepatology 2009;50:185–197.

[35] **Berres ML**, **Koenen RR**, Rueland A, Zaldivar MM, Heinrichs D, Sahin H, et al. Antagonism of the chemokine Ccl5 ameliorates experimental liver fibrosis in mice. J Clin Invest 2010;120:4129–4140.

[36] **Gadd VL**, **Melino M**, Roy S, Horsfall L, O'Rourke P, Williams MR, et al. Portal, but not lobular, macrophages express matrix metalloproteinase-9: association with the ductular reaction and fibrosis in chronic hepatitis C. Liver Int 2013;33:569–579.

[37] **Lee J**, **Kim CM**, Cha JH, Park JY, Yu YS, Wang HJ, et al. Multiplexed digital spatial protein profiling reveals distinct phenotypes of mononuclear phagocytes in livers with advanced fibrosis. Cells 2022;11:3387.

[38] **Jiao J**, **Sanchez JI**, Saldarriaga OA, Solis LM, Tweardy DJ, Maru DM, et al. Spatial molecular and cellular determinants of STAT3 activation in liver fibrosis progression in non-alcoholic fatty liver disease. JHEP Rep 2023;5:100628.

[39] Mi H, Ho WJ, Yarchoan M, Popel AS. Multi-scale spatial analysis of the tumor microenvironment reveals features of cabozantinib and nivolumab efficacy in hepatocellular carcinoma. Front Immunol 2022;13:892250.

[40] **Ding GY**, **Ma JQ**, **Yun JP**, **Chen X**, Ling Y, Zhang S, et al. Distribution and density of tertiary lymphoid structures predict clinical outcome in intrahepatic cholangiocarcinoma. J Hepatol 2022;76:608–618.

[41] **Lu LG**, **Zhou ZL**, **Wang XY**, Liu BY, Lu JY, Liu S, et al. PD-L1 blockade liberates intrinsic antitumourigenic properties of glycolytic macrophages in hepatocellular carcinoma. Gut 2022;71:2551–2560.

[42] Krenkel O, Puengel T, Govaere O, et al. Therapeutic inhibition of inflammatory monocyte recruitment reduces steatohepatitis and liver fibrosis. Hepatology Apr 2018;67(4):1270–1283.

[43] **Yue F**, **Cheng Y**, **Breschi A**, **Abhdalla AT**, **Mossanen JC**, **Kohlhepp M**, et al. A comparative encyclopedia of DNA elements in the mouse genome. Nature 2014;515:355–364.

[44] Jiang C, Li P, Ruan X, Ma Y, Kawai K, Suemizu H, et al. Comparative transcriptomics analyses in livers of mice, humans, and humanized mice define human-specific gene networks. Cells 2020;9:2566.